

Overlapped grouping measurement: A unified framework for measuring quantum states

Bujiao Wu^{1,2}, Jinzhao Sun^{3,1}, Qi Huang^{4,1}, and Xiao Yuan^{1,2}

¹Center on Frontiers of Computing Studies, Peking University, Beijing 100871, China

²School of Computer Science, Peking University, Beijing 100871, China

³Clarendon Laboratory, University of Oxford, Parks Road, Oxford OX1 3PU, United Kingdom

⁴School of Physics, Peking University, Beijing 100871, China

January 11th 2023

Quantum algorithms designed for realistic quantum many-body systems, such as chemistry and materials, usually require a large number of measurements of the Hamiltonian. Exploiting different ideas, such as importance sampling, observable compatibility, or classical shadows of quantum states, different advanced measurement schemes have been proposed to greatly reduce the large measurement cost. Yet, the underline cost reduction mechanisms seem distinct from each other, and how to systematically find the optimal scheme remains a critical challenge. Here, we address this challenge by proposing a unified framework of quantum measurements, incorporating advanced measurement methods as special cases. Our framework allows us to introduce a general scheme — overlapped grouping measurement, which simultaneously exploits the advantages of most existing methods. An intuitive understanding of the scheme is to partition the measurements into overlapped groups with each one consisting of compatible measurements. We provide explicit grouping strategies and numerically verify its performance for different molecular Hamiltonians with up to 16 qubits. Our numerical result shows significant improvements over existing schemes. Our work paves the way for efficient quantum measurement and fast quantum processing with current and near-term quantum devices.

1 Introduction

How to efficiently measure a quantum state is a fundamental problem with great practical relevance. Algorithms tailored for noisy intermediate-scale quantum (NISQ) devices [4, 9, 20, 53] usually require measuring complicated multi-qubit observables, such as the Hamiltonian [5, 7, 12–14, 19, 21, 22, 25, 28, 29, 32, 38–43, 45, 47, 48, 50, 52, 60, 66, 68, 69, 72, 73, 78]. When decomposing the Hamiltonian into local measurable observables, it may contain a large number of terms. For example, an electronic Hamiltonian with Coulomb interaction generally has $\mathcal{O}(M^4)$ terms when represented with M fermionic modes [3, 7, 43, 54]. The number of terms could already become quite large when we consider the classical

Bujiao Wu: These two authors contributed equally

Jinzhao Sun: These two authors contributed equally

Xiao Yuan: xiaoyuan@pku.edu.cn

limit with a large M , where the naive strategy of equally measuring all the observables requires a prohibitively long time. We also need error mitigation techniques to suppress calculation errors, which again introduces a large sample overhead with increasing problem size [6, 17, 18, 23, 39, 45, 46, 51, 57, 59, 61]. Therefore, an efficient quantum measurement scheme is crucial for demonstrating a clear and robust quantum advantage with NISQ devices.

Without introducing additional entangling circuits, three types of advanced measurement schemes have been proposed to reduce the measurement cost by exploiting different features of the to-be-measured observables [11, 15, 16, 27, 31, 33, 38, 62, 63, 65, 67]. First, observables may have different weight coefficients and we can exploit importance sampling to distribute more measurements to observables with large weights [44, 67]. Next, observables may be compatible with some other ones, in the sense that they could be simultaneously measured with the same measurement basis. We can thus group observables into sets of compatible observables using fewer measurements [16, 28, 35, 38, 50, 64, 65, 76]. Another notable but conceptually different scheme considers classical shadows of quantum states using uniformly random local measurements, which are extensively investigated in theoretical and experimental works [1, 2, 10, 31, 58, 74, 77]. By properly post-processing the classical measurement outcomes, one can simultaneously obtain the expectation values of any observables. The cost of the original uniform classical shadow scheme [31] scales exponentially to the number of qubits that the observable non-trivially acts on, and later LBCS and derandomized CS methods were further proposed to reduce the measurement cost [27, 33]. While the optimized classical shadow method outperforms the other two types of methods in numerical experiments, how they are related, and how to find an optimized method that exploits the advantages of all these advanced measurement schemes remain open.

Here, we address these problems in quantum state measurement. We first introduce a unified framework that integrates the advantages of the typically advanced measurement schemes in Sec. 2. In particular, we show how to understand the classical shadow method as a generalized observable grouping method. We next introduce the overlapped grouping measurement scheme that simultaneously exploits the features of the importance sampling, observable compatibility, and classical shadows in Sec. 3. While finding the optimal overlapped groups could be computationally challenging, we provide explicit algorithms that output an optimized measurement scheme in Sec. 4. We then numerically benchmark our method in Sec. 5 by comparing it to existing advanced works [27, 31, 33, 38, 65] in estimating expectations of molecular Hamiltonians, as a subroutine in most quantum algorithms. Our numerical result shows prominent improvements over all the others. The proposed method is immediately applicable to currently available and near-future quantum computing experiments. In Sec. 6, we conclude this work and suggest some interesting future investigations.

2 A unified framework

Now we introduce a framework for measuring hermitian objective observables $\mathbf{O} := \sum_j \alpha_j Q^{(j)}$ on a multi-qubit quantum state ρ . Here $Q^{(j)} \in \{I, X, Y, Z\}^n$ are tensor products of single-qubit Pauli operators, and we also call $Q^{(j)}$ local Pauli strings. Naively, we could measure each term $Q^{(j)}$ to obtain the expectation value, $\text{tr}(\rho Q^{(j)})$, and hence the expectation value of the objective observable, $\text{tr}(\rho \mathbf{O})$, whereas more efficient schemes may be found by exploiting the properties of the objective observables.

We first consider observable compatibility. Let Q and R be tensor products of single-

qubit Pauli operators $Q = \bigotimes_{i=1}^n Q_i$ and $R = \bigotimes_{i=1}^n R_i$ with $Q_i, R_i \in \{I, X, Y, Z\}$. We let $Q \triangleright R$ denote $Q_i = R_i$ or $Q_i = I$ for any i , indicating that measuring observable R equivalently measures Q . We say that Q is *compatible* with R when $Q_i \triangleright R_i$ or $R_i \triangleright Q_i$ for any i , meaning that Q and R can be simultaneously measured. In an extreme case, when each operator $Q^{(j)}$ is compatible with the same Pauli basis P , we can simultaneously obtain all the expectation value $\text{tr}(\rho Q^{(j)})$ by measuring one basis P . Nevertheless, a practical case generally consists of observables that are compatible with only a subset of other observables. Then we need to find a set of Pauli bases $\{P\}$ such that each observable $Q^{(j)}$ is compatible with at least one Pauli basis. After choosing the Pauli bases $\{P\}$, the next question is how to distribute the measurement samples to each basis P , which corresponds to the idea of importance sampling. Without loss of generality, we select each basis P randomly with the probability $\mathcal{K}(P)$.

Now, suppose that we have determined $\{(P, \mathcal{K}(P))\}$, and we can define an estimator

$$\hat{v} = \sum_j \alpha_j f(P, Q^{(j)}, \mathcal{K}) \mu(P, \text{supp}(Q^{(j)})), \quad (1)$$

where $\text{supp}(Q) := \{i | Q_i \neq I\}$ is the support of Q , $\mu(P, \text{supp}(Q^{(j)})) := \prod_{i \in \text{supp}(Q^{(j)})} \mu(P_i)$, and $\mu(P_i)$ is the single-shot outcome by measuring the i th qubit with single-qubit Pauli operator P_i . Here, $\mu(P, \text{supp}(Q^{(j)}))$ effectively gives measurement results of $Q^{(j)}$ obtained from measuring with the basis P . $f(P, Q^{(j)}, \mathcal{K})$ is associated with the probability distribution \mathcal{K} of measurement P and $Q^{(j)}$, which is designed to guarantee that \hat{v} is an unbiased estimation of $\text{tr}(\rho \mathbf{O})$. It depends on the measurement scheme, and we will show its explicit form for different schemes later. Assuming that $\mathbb{E}[f(P, Q^{(j)}, \mathcal{K})] = 1$, we will show that $\mathbb{E}[\hat{v}] = \text{tr}(\rho \mathbf{O})$, i.e., \hat{v} is an unbiased estimator of the observable expectation $\text{tr}(\rho \mathbf{O})$ in the following proposition.

Proposition 1. *Let $\mathbf{O} = \sum_j \alpha_j Q^{(j)}$ where $Q^{(j)}$ are local Pauli strings, and \hat{v} be defined as in Eq. (1) with $\mathbb{E}[f(P, Q^{(j)}, \mathcal{K})] = 1$, then \hat{v} is an unbiased estimation of $\text{tr}(\rho \mathbf{O})$.*

Proof. By the definition of \hat{v} , we have

$$\begin{aligned} \mathbb{E}[\hat{v}] &= \mathbb{E} \left[\sum_j \alpha_j f(P, Q^{(j)}, \mathcal{K}) \mu(P, \text{supp}(Q^{(j)})) \right] \\ &= \sum_j \alpha_j \mathbb{E}_P [f(P, Q^{(j)}, \mathcal{K})] \mathbb{E}_{\mu|P} [\mu(P, \text{supp}(Q^{(j)}))] \\ &= \sum_j \alpha_j \text{tr}(\rho Q^{(j)}) = \text{tr}(\rho \mathbf{O}) \end{aligned} \quad (2)$$

where the first equation holds because of the conditional expectation formula. \square

In the following, we give explicit expressions of $f(\cdot, \cdot, \cdot)$ for different existing measurement schemes.

(1) *Importance sampling.* The strategy of the importance sampling measures each observable $Q^{(j)}$ independently with the basis $P^{(j)} = Q^{(j)}$, and the associated probability distribution is determined by the weight of the observable as $\mathcal{K}(P^{(j)}) = |\alpha_j| / \|\alpha\|_1$ with $\|\alpha\|_1 = \sum_{j=1}^m |\alpha_j|$ being the l_1 norm of $\alpha = (\alpha_1, \dots, \alpha_m)$, and f defined as

$$f_{l_1}(P, Q^{(j)}, \mathcal{K}) = \mathcal{K}(P)^{-1} \delta_{P, Q^{(j)}}. \quad (3)$$

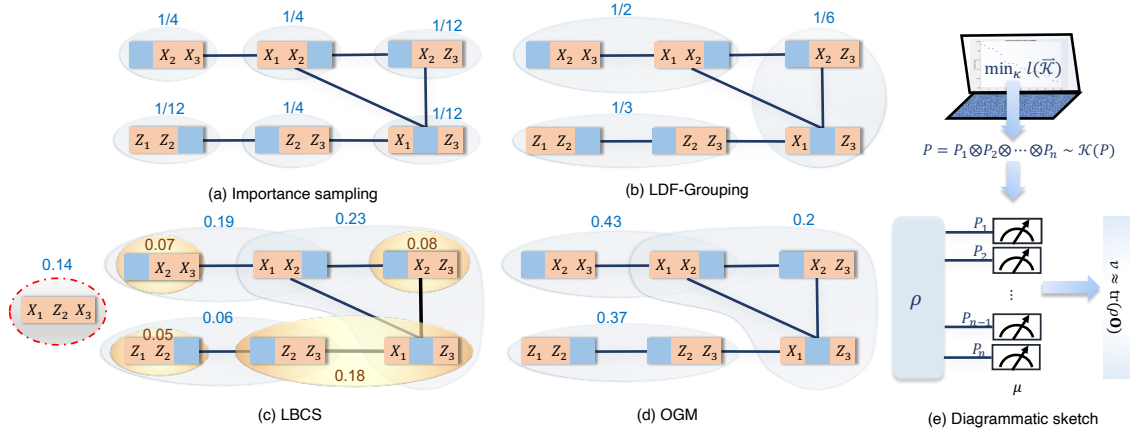


Figure 1: An illustrative example of the (a) l_1 -sampling, (b) LDF-grouping, (c) LBCS, and (d) OGM methods. A vertex represents an observable, and an edge is connected between two vertices when they are compatible. The light blue (yellow) set represents a Pauli measurement basis. Different measurement schemes correspond to different light blue (yellow) sets with different probabilities. Here we consider an example of measuring $\mathbf{O} = X_1 X_2 / 4 + X_2 X_3 / 4 + X_2 Z_3 / 12 + Z_2 Z_3 / 4 + Z_1 Z_2 / 12 + X_1 Z_3 / 12$ with a 3-qubit state $|\psi\rangle = |000\rangle / \sqrt{2} + |111\rangle / \sqrt{2}$. The variance for importance sampling, LDF-grouping, LBCS and OGM algorithms of this instance are 0.90, 0.56, 0.74, 0.50, respectively. (e) Schematic diagram of the unified framework. We first determine the set of Pauli basis $\{P\}$ and the probability distributions $\{\mathcal{K}(P)\}$ using Algorithm 1. We next measure the quantum state ρ with a different Pauli basis drawn from the distribution \mathcal{K} and post-process the measurement outcomes to obtain the estimation of $\text{tr}(\rho \mathbf{O})$.

It is easy to check that $\mathbb{E}_P \left[f_{l_1} \left(P, Q^{(j)}, \mathcal{K} \right) \right] = 1$. This method is also referred to as l_1 -sampling, since the sampling probability is associated with the l_1 -norm of $Q^{(j)}$. The l_1 -sampling needs $\mathcal{O}(\|\alpha\|_1^2 / \varepsilon^2)$ copies of quantum states ρ to approximate the expectation of \mathbf{O} with an additive error ε . The number of copies is obtained from Chebyshev inequality, and we leave details of error analysis in Appendix A.

(2) *Grouping*. The grouping method exploits observable compatibility by partitioning the observables $\mathcal{O} = \{Q^{(j)}\}$ into several non-overlapped sets $\mathcal{S} = \{e_1, \dots, e_s\}$ such that $e_j \cap e_{j'} = \emptyset$ ($\forall j \neq j'$), $\cup_j e_j = \mathcal{O}$. It also requires that observables in the same set are compatible with each other, such that there exists a measurement basis $P^{(j)}$ satisfying $Q \triangleright P^{(j)}, \forall Q \in e_j$. Let $\mathcal{K}(P^{(j)})$ be the probability that $P^{(j)}$ is selected. It could be optimized using the importance sampling by setting $\mathcal{K}(P^{(j)})$ proportional to the total weight of the observables in the set $P^{(j)}$ as $\mathcal{K}(P^{(j)}) = \|e_j\|_1 / \|\alpha\|_1$. Here the weight of a set e_j is defined as the l_1 -norm of the weights of the observables in this set as $\|e_j\|_1 = \sum_{Q^{(k)} \in e_j} |\alpha_k|$. The function f for the optimized grouping method is

$$f_{\text{Group}} \left(P^{(j)}, Q^{(k)}, \mathcal{K} \right) = \mathcal{K}(P^{(j)})^{-1} \delta_{Q^{(k)} \in e_j}. \quad (4)$$

where $\delta_{P, Q^{(j)}}$ equals one if $P = Q^j$ and equals zero otherwise. Then we have

$$\mathbb{E}_P \left[f_{\text{Group}} \left(P, Q^{(k)}, \mathcal{K} \right) \right] = \sum_j \mathcal{K} \left(P^{(j)} \right) \mathcal{K} \left(P^{(j)} \right)^{-1} [Q^{(j)} \in e_j] = 1. \quad (5)$$

The number of copies of quantum states ρ needed here is associated with the grouping strategy, and we give an explicit upper bound for the number of copies requiring to approximate $\text{tr}(\rho \mathbf{O})$ with an additive error ε for any given grouping strategy in Appendix A.

Finding the exact minimum number of groups has been proved to be NP-hard [37]. Several heuristic algorithms, such as the *largest degree first* (LDF) method [65] have been proposed to give approximate solutions. We refer to Appendix B for a detailed implementation of the heuristic grouping method.

(3) *Classical shadows*. The conventional classical shadow (CS) method measures the quantum state with a random Pauli basis, which corresponds to a Pauli string $P \in \{X, Y, Z\}^{\otimes n}$ within our framework. The original scheme in the seminal work [31] considers a uniform probability $\mathcal{K}(P) = 1/3^n$ whereas the locally biased classical shadow (LBCS) method [27] assumes a general product distribution $\mathcal{K}(P) = \prod_i \mathcal{K}_i(P_i)$. The function f_{CS} is

$$f_{\text{CS}}(P, Q^{(j)}, \mathcal{K}) = \prod_i f_i(P_i, Q_i^{(j)}, \mathcal{K}_i), \quad (6)$$

with $f_i(P_i, Q_i^{(j)}, \mathcal{K}_i) = \delta_{Q_i, I} + \mathcal{K}_i(P_i)^{-1} \delta_{Q_i^{(j)}, P_i}$. One can check that

$$\mathbb{E}_P [f_{\text{CS}}(P, Q^{(j)}, \mathcal{K})] = \prod_i \sum_{P_i} \mathcal{K}(P_i) f_i(P_i, Q_i^{(j)}, \mathcal{K}_i) = 1. \quad (7)$$

The number of copies ρ to approximate the expectation of \mathbf{O} with an additive error ε and $1 - \delta$ success probability is bounded to $O\left(3^{\text{local}(\mathbf{O})} \left(\sum_{j=1}^m \alpha_j\right)^2 / (\delta \varepsilon^2)\right)$, where $\text{local}(Q^{(j)}) := \#\{k | Q_k^{(j)} \neq \mathbb{I}\}$ is the maximum number of qubits k such that $Q_k^{(j)}$ is not identity for all of j . We refer to Appendix A for detailed proof.

(4) *Derandomized CS*. Recently, Huang, Kueng and Preskill [33] proposed a derandomized classical shadow algorithm, which shows great practical performance compared with conventional classical shadow methods. The derandomization algorithm first assigns a collection of T completely random n -qubit Pauli measurements, and then derandomizes the process for sampling measurement set \mathcal{P} by greedily and adaptively choosing current $P^{(j)}$ in the j -th step, provided derandomized measurements $P^{(1)} \dots P^{(j-1)}$, that minimizes the conditional expected value over all remaining random measurement assignments. Given all the selected measurements \mathcal{P} , the estimator of the derandomized CS algorithm can be expressed as

$$\hat{v} = \sum_j \alpha_j \frac{1}{\sum_{P \in \mathcal{P}} \delta_{Q^{(j)} \triangleright P}} \sum_{P: Q^{(j)} \triangleright P} \mu(P, \text{supp}(Q^{(j)})) \quad (8)$$

within our framework. Now we give a sampling version for this method and prove that it can also be unified to the unified framework, as shown in Eq. (1).

For the measurement sequence $P^{(1)}, \dots, P^{(T)}$, suppose the frequency of $P^{(k)}$ be t_k , let $p_k = t_k/T$ be the probability to select $P^{(k)}$, and denote this distribution as \mathcal{K} . Then proposition 1 still holds as long as for any observable $Q^{(j)}$ where $j \in [m]$, there exists a measurement $P^{(k)}$ in the measurement sequence such that $Q^{(j)} \triangleright P^{(k)}$. In this case, we can rewrite Eq. (8) as

$$\hat{v} = \sum_j \alpha_j \frac{1}{p(Q^{(j)})} \mu(P^{(k)}, \text{supp}(Q^{(j)})) \quad (9)$$

for a selected measurement $P^{(k)}$, where $p(Q^{(j)})$ is the probability to measure $Q^{(j)}$. It is easy to check that $\mathbb{E}[f(P^{(k)}, Q^{(j)}, \mathcal{K})] = \mathbb{E}\left[\frac{1}{p(Q^{(j)})}\right] = 1$, and hence $\mathbb{E}[\hat{v}] = \text{tr}(\rho \mathbf{O})$.

In Fig. 1, we show explicit examples of the above three typical methods. While Ref. [27] showed the superiority of the LBCS method, we can see that LBCS essentially exploits an alternative view of observable compatibility, which is captured by the unified framework.

However, since the measurements are selected locally in LBCS, we have to measure redundant observables, such as $X_1 Z_2 X_3$ in our example of Fig. 1. This term has no contribution to the objective observable, but is still assigned a certain number of measurements. For a general observable, many measurements might be assigned to these redundant terms, and thus makes LBCS non-optimal or even costly with increasing system size.

3 Overlapped grouping measurement

Here, we propose a new scheme that exploits the advantages of the aforementioned typical measurement methods. We first introduce the concept of *overlapped grouping* and then give a comparison of this strategy and other existing strategies.

3.1 Overlapped grouping

Definition 1 (Overlapped grouping). *For a set of observables $\mathcal{O} = \{Q^{(j)}\}$, the collection $\mathcal{S} = \{e_1, \dots, e_s\}$ is an overlapped grouping when $\cup_j e_j = \mathcal{O}$ with corresponding measurements $\{P^{(1)}, \dots, P^{(s)}\}$ satisfying $Q \triangleright P^{(j)}, \forall Q \in e_j$.*

Suppose that we have determined the probabilities $\{\mathcal{K}(P^{(j)})\}$, and we can define a new function f for the overlapped grouping as

$$f_G(P, Q, \mathcal{K}) = \chi(Q)^{-1} \delta_{Q \triangleright P}, \quad (10)$$

where $\chi(Q) := \sum_{P: Q \triangleright P} \mathcal{K}(P)$ represents the probability that Q is effectively measured with the basis P . Now we can define

$$\hat{v}_G = \sum_j \alpha_j f_G(P, Q^{(j)}, \mathcal{K}) \mu(P, \text{supp}(Q^{(j)})) \quad (11)$$

as an unbiased estimator of $\text{tr}(\rho \mathbf{O})$. Intuitively, an unbiased estimation of $\text{tr}(\rho Q^{(j)})$ can be generated from the measured results of $Q^{(j)}$ divided by its measured probability. From the definition of f_G , we have $\mathbb{E}_P[f_G(P, Q, \mathcal{K})] = \sum_{P: Q \triangleright P} \mathcal{K}(P) \frac{1}{\chi(Q)} = 1$, and hence \hat{v}_G is also an unbiased estimation of $\text{tr}(\rho \mathbf{O})$ by Proposition 1. To summarise, an overlapped grouping measurement (OGM) scheme works as follows.

- S1. Find the overlapped sets \mathcal{S} with corresponding measurements $\{P^{(1)}, \dots, P^{(s)}\}$.
- S2. Find the probability distribution $\{\mathcal{K}(P^{(j)})\}$.
- S3. Measure the quantum state with a randomly generated basis P and process the outcomes with Eq. (1) and (10).

A specific OGM scheme is determined by the choice of sets \mathcal{S} (equivalently $\{P^{(j)}\}$) and the probability distribution $\{\mathcal{K}(P^{(j)})\}$. To quantify the performance of the scheme, we consider the variance of the estimator, as shown in the following proposition.

Proposition 2. *The variance of \hat{v}_G defined in Eq. (11) is*

$$\text{Var}(\hat{v}_G) = \sum_{j,k} \alpha_j \alpha_k g(Q^{(j)}, Q^{(k)}) \text{tr}(\rho Q^{(j)} Q^{(k)}) - \text{tr}(\rho \mathbf{O})^2 \quad (12)$$

where $g(Q^{(j)}, Q^{(k)}) := \chi^{-1}(Q^{(j)}) \chi^{-1}(Q^{(k)}) \sum_{P: Q^{(j)} \triangleright P \wedge Q^{(k)} \triangleright P} \mathcal{K}(P)$.

Proof. Since $\text{Var}(\hat{v}_G) = \mathbb{E}[\hat{v}_G^2] - \mathbb{E}[\hat{v}_G]^2$, Proposition 2 follows from the following equations

$$\begin{aligned}\mathbb{E}_P[f_G(P, Q, \mathcal{K})f_G(P, R, \mathcal{K})] &= \frac{\sum_{P: Q \triangleright P \wedge R \triangleright P} \mathcal{K}(P)}{\chi(Q)\chi(R)}, \\ \mathbb{E}_{\mu(P|Q, R)}[\mu(P, \text{supp}(Q))\mu(P, \text{supp}(R))] &= \text{tr}(\rho QR),\end{aligned}\tag{13}$$

where the first equation holds directly by its definition and the second equation holds because we have $\mu(P, \text{supp}(Q))\mu(P, \text{supp}(R)) = \mu(P, \text{supp}(Q \oplus R)) = \mu(P, \text{supp}(QR))$ when $Q, R \in \{I, X, Y, Z\}^n$. \square

The variance determines the sample complexity. In particular, we need the total number of measurements $T \geq \text{Var}(\hat{v}_G) / (\delta \varepsilon^2)$ samples to achieve $\Pr[|\hat{v}_G - \text{tr}(\rho \mathbf{O})| \geq \varepsilon] \leq \delta$ with error $\varepsilon \geq 0$ and failure probability $\delta \in [0, 1]$.

3.2 Illustration and comparison with other measurement schemes

We illustrate the differences between our OGM scheme and other measurement schemes in Fig. 1. As illustrated in Fig. 1, importance sampling selects an observable in each iteration, and measures the prepared state with the sampled observables to obtain the estimations associated with this observable. Grouping strategy leverages the compatible property of the observables, and measures the observables that are compatible jointly. Nevertheless, it only exploits a very limited space of the full probability space for 4^n possible measurements in $\{I, X, Y, Z\}^n$. Moreover, for the sake of the grouping determination using the heuristic strategy, an observable can not arise in two different sets. Therefore, it might be inefficient in leveraging of the measurements. Classical shadow method finds the optimized probabilities of each qubit of the measurement, and it also measures the observables jointly. However, since the CS method independently generates Pauli operators on each qubit, it will generate useless measurements, such as $X_1 Z_2 X_3$ in Fig. 1(c). As a comparison, for any measurement P in set $\{P^{(1)}, \dots, P^{(s)}\}$ generated from the OGM scheme, there exists at least an observable $Q^{(j)}$, such that $Q^{(j)} \triangleright P$.

The overlapped grouping measurement framework defined as in Eq. (10) without an explicit assignment of $\{P^{(k)}\}$ and \mathcal{K} covers importance sampling, LDF Grouping, CS and the “probabilistic version” of the derandomized CS algorithm as in Eq. (9). The importance sampling, grouping and CS algorithms can be regarded as a special OGM framework with some restrictions for the distribution of measurements $\{(P, \mathcal{K}(P))\}$. We note that in our method $f_G(P, Q, \mathcal{K}) = \chi(Q)^{-1} \delta_{Q \triangleright P}$ may lead to more effective data post-processing since it exploits all the compatible properties of observables in the overlapped sets, and the “probabilistic version” estimation in Eq. (9) of the derandomized CS algorithm also belongs to this scope, since it is equivalent to the estimation expression with the OGM grouping strategy in Eq. (11).

We can also observe that OGM is strictly better than the classical shadow method. The OGM scheme reduces to the CS method when we choose $P^{(j)} \in \{X, Y, Z\}^{\otimes n}$ and restrict the probability distribution $\mathcal{K}(P^{(j)})$ to have a local product structure on different qubits. We remark that OGM will not measure redundant observables as that in the local shadow methods.

The estimator in Eq. (8) indicates that derandomization utilizes the compatible properties of observables when measuring on the predetermined basis. Once the measurement bases are determined, it could be regarded as a special overlapped grouping method.

In OGM, challenges remain to (1) determine the collection \mathcal{S} and (2) find the probability distributions \mathcal{K} . Similar to the case of grouping method, finding the optimal overlapped

groups given the objective observables is also NP-hard. In Sec. 4, we develop an explicit strategy to determine an approximate solution \mathcal{S} by leveraging a greedy algorithm based on the weights of the observables. To find the probability distribution \mathcal{K} , we apply an optimization procedure to adaptively search for the solution that minimizes the estimator variance.

4 Explicit grouping strategies

We show in Algorithm 1 our strategy to determine the overlapped sets $\mathbf{e}_1, \dots, \mathbf{e}_s$ and the associated probability $\mathcal{K}_j := \mathcal{K}(P^{(j)})$. The main idea is that under the premise of covering all the objective observables, we add an observable which has not been accessed into a new set, and add all compatible observables into this set. We give priority to observables with larger absolute weights since it has more contributions to the estimation. We note that different sequences to add a new observable into an existing set will influence the structure of sets and the number of sets. Algorithm 1 provides a grouping strategy by adding a new observable by its importance (weight) and trying to reduce the number of sets as far as possible. Meanwhile, the procedure guarantees that whenever an observable $Q^{(j)}$ is compatible with the measurement $P^{(i)}$, it is in the set \mathbf{e}_i . See Appendix C for an alternative strategy, which has slightly better performance however based on a more dedicated optimization procedure.

Algorithm 1: Overlapped set generation.

Input : n, m and $Q^{(1)}, \dots, Q^{(m)}, \alpha_1, \dots, \alpha_m$.
Output: $\{P^{(s)}\}$ with initial probabilities $\{\mathcal{K}_s\}$.

- 1 *Sorting $\{Q^{(j)}\}$ to the descending order according to their weights $|\alpha_j|$;*
- 2 $j \leftarrow 1$ and $s \leftarrow 1$;
- 3 **while** $\exists Q^{(j)}$ that is not in any sets :
- 4 *Let $Q^{(j)}$ be the first observable in the sorted sequence which has never appeared in any sets and add it into a new set \mathbf{e}_s ;*
- 5 $s \leftarrow s + 1$;
- 6 *Initialize the measurement of \mathbf{e}_s as $P^{(s)} \leftarrow Q^{(j)}$;*
- 7 **for** $k \leftarrow j + 1$ **to** m :
- 8 **if** observable $Q^{(k)}$ is compatible with $P^{(s)}$:
- 9 *Add $Q^{(k)}$ into set \mathbf{e}_s ;*
- 10 *Update $P^{(s)}$ to $P^{(s)} \vee Q^{(k)}$;* /* $P = Q \vee R$ is
- 11 *defined as $P_i = Q_i$ if $Q_i = R_i$ and $P_i = Q_i R_i$ otherwise. */*
- 11 *Let the initial probability of $P^{(s)}$ be the summation of the weight of all observables in this set;*
- 12 **for** $k \leftarrow 1$ **to** $j - 1$:
- 13 **if** observable $Q^{(k)}$ is compatible with $P^{(s)}$:
- 14 *Add $Q^{(k)}$ into set \mathbf{e}_s , and update $P^{(s)}$ to $P^{(s)} \vee Q^{(k)}$;*

The algorithm outputs the measurements $\{P\}$ with non-optimized probabilities $\{\mathcal{K}\}$. Here the initial probability of $P^{(s)}$ is not chosen as the weight of \mathbf{e}_s since we wish to distinguish the importance of different sets and give more priority to the sets which are generated in front of \mathbf{e}_s . We can then optimize $\{\mathcal{K}\}$ to further minimize the estimator variance. However, the variance $\text{Var}(\hat{v}_G)$ in Eq. (12) depends on the input state ρ , which could be unknown in general. Alternatively, we consider the diagonal approximation of

$\text{Var}(\hat{v}_G)$ (see similar techniques in Ref. [27]), which is explicitly expressed as

$$l(\vec{\mathcal{K}}) = \sum_j \frac{\alpha_j^2}{\chi(Q^{(j)}, \vec{\mathcal{K}})}, \quad (14)$$

where $\chi(Q, \vec{\mathcal{K}}) = \sum_{P: Q \in P} \mathcal{K}(P)$ and $\vec{\mathcal{K}} := (\mathcal{K}_1, \dots, \mathcal{K}_s)$ represents all the corresponding probabilities. We give the mathematical supports that why we utilize $l(\vec{\mathcal{K}})$ as the cost function in Appendix E. There are several advantages of using the diagonal approximation $l(\vec{\mathcal{K}})$ instead of the actual variance — (1) independence of the quantum state, (2) fast classical evaluation, (3) including dominant contribution to the variance since $\text{tr}(\rho Q^{(j)} Q^{(k)}) < \text{tr}(\rho Q^{(j)} Q^{(j)}) = 1$ when $j \neq k$. Therefore, we could instead regard $l(\vec{\mathcal{K}})$ as the cost function and minimize it by optimizing over $\vec{\mathcal{K}}$. From the expression of $l(\vec{\mathcal{K}})$ in Eq. (14), we see the cost function is not convex in $\vec{\mathcal{K}}$ and hence there is no closed minimum solution. An estimation can be generated by searching for a local minimum solution of the cost function in Eq. (14). To further give a better estimation and avoid being trapped into bad local minima, we slightly revise the cost function, as shown in the following subsection.

4.1 Optimization process

For the optimization process of the OGM method, we will further speed it up by adaptively deleting the groups that have very small initial probabilities until the cost function stops decreasing with the disturbance. Note that after cutting down the groups with small weights, some observables with small coefficients will disappear in the cost function. Therefore, we adjust the final cost function as

$$l(\vec{\mathcal{K}}) = \sum_{Q^{(j)} \in \mathcal{S}} \frac{\alpha_j^2}{\chi(Q^{(j)})} + \sum_{Q^{(j)} \notin \mathcal{S}} \alpha_j^2 T, \quad (15)$$

where T is the total number of samples, $Q^{(j)} \in \mathcal{S}$ if there exists a set \mathbf{e} such that $Q^{(j)} \in \mathbf{e}$, and $\sum_{Q^{(j)} \notin \mathcal{S}}$ is the penalty caused by deleting some sets. The selection of the final cost function in Eq. (15) is inspired by the relationship between the variance and the number of samples. More specifically, Chebyshev inequality $T \geq \text{Var}(\hat{v}) / (\delta \varepsilon^2)$ indicates that $\text{Var}(\hat{v})$ is linear in T . Hence we introduce $\alpha_j^2 T$ to compensate the initial error ε_0 for excluding the observable $Q^{(j)}$. The initial error $\varepsilon_0 = \left| \sum_{j: Q^{(j)} \notin \mathcal{S}} \alpha_j \text{tr}(\rho Q^{(j)}) \right|$ implies biases of our estimation. We could search for an optimized T in a real experiment with a small-scaled input size with an initial T_0 . Since the cost function in Eq. (15) is not convex, we could find a local minimum solution using the nonconvex optimization methods.

Since our OGM method assumes measurements drawn from the probability distribution, the measurement accuracy may fluctuate. We will derandomize the scheme by fixing almost all of the choices of measurements P in the next subsection.

4.2 Sampling strategy

Suppose that we have determined the measurement basis sets $\mathbf{e}_1, \dots, \mathbf{e}_s$ and the optimized probability distribution $\{(P, \mathcal{K}(P))\}$ using the above strategy. In practical computation, we usually have constraints on the maximum allowed number of measurements. In what follows, we provide a partially derandomized strategy with the given number of measurements T . For the j th measurement $P^{(j)}$ with sampling probability \mathcal{K}_j , we choose $\lfloor T \mathcal{K}_j \rfloor$

number of measurements for $P^{(j)}$, and select an additional one $P^{(j)}$ with probability $T\mathcal{K}_j - \lfloor T\mathcal{K}_j \rfloor$, as shown in the Algorithm 2.

Algorithm 2: Partially derandomized sampling process for OGM.

Input : Measurements $P^{(1)}, \dots, P^{(s)}$, which follows distribution $\mathcal{K} = \{\mathcal{K}_1, \dots, \mathcal{K}_s\}$, the number of selected measurements T .
Output: List \mathcal{M} which contains selected measurements.

- 1 *Sorting measurements $P^{(1)}, \dots, P^{(s)}$ to descending order in terms of its probabilities;*
- 2 **for** $j \leftarrow 1$ **to** s
- 3 *Add $\lfloor \mathcal{K}_j T \rfloor$ number of $P^{(j)}$ into list \mathcal{M} ;*
- 4 $\mathcal{K}_j \leftarrow \mathcal{K}_j T - \lfloor \mathcal{K}_j T \rfloor$;
- 5 **for** $j \leftarrow 1$ **to** s *and* $\text{size}(\mathcal{M}) < T$
- 6 *Add one $P^{(j)}$ into list \mathcal{M} with probability \mathcal{K}_j ;*
- 7 **return** \mathcal{M} ;

Observe that the estimation \hat{v}_G does not rely on the arrangement of measurements. Let \mathcal{M} be the list for the selected measurements, and note here we allow a measurement to appear more than once in the list \mathcal{M} . It is easy to check the expectation number of samples for $P^{(j)}$ is equal to $\mathcal{K}_j T$ with Algorithm 2. Note that in Algorithm 2, the number of sampled measurements may not exactly equal T , although it is close to T if $s \ll T$. Hence in the numerical experiment we additionally add $P^{(j)}$ to \mathcal{M} for the measurement $P^{(j)}$ satisfies $\mathcal{K}_j T < 1$ and $\text{size}(\mathcal{M}) < T$ in the descending sequence sorted in Step (1) of Algorithm 2 if the size of \mathcal{M} is less than T . We provide detailed discussions on the variance of the partially derandomized strategy in Appendix D.

5 Numerical tests

In this section, we numerically demonstrate the overlapped grouping measurement algorithms for the energy estimation of molecular systems, and compare our methods with other advanced measurement strategies, including LDF-grouping, locally biased classical shadows, and derandomized classical shadows. We do not include importance sampling method in the comparison since its performance is worse than others. Algorithm 3 gives the full estimation process for the OGM algorithm. In Step 2 of Algorithm 3, we begin the optimization process from a better initialized probabilities by picking the distribution with the minimum cost function from uniformly randomly selected 10 distributions around the initialized distribution \mathcal{K}_s from Step 1. To show the robust advantages of the OGM algorithm, we directly choose the probabilities initialized in Algorithm 1 without performing Step 2 to give the optimized measurement distributions, and outputs the errors for estimations with 1000 samples in Table 1.

We compare the measurement schemes for different molecular Hamiltonians, ranging from 4 to 16 qubits. We first consider the molecular Hamiltonian measurement on the ground state of molecular Hamiltonians, in which the fermionic Hamiltonians are mapped to the qubit ones under the Jordan-Wigner (JW) transformation and the number of terms in the molecular Hamiltonians scales quartically to the system size. In practice, the cost function in Eq. (14) might lead to the optimized result for the probability distributions trapped in the local minimum. Here, we address this problem by adding an additional disturbance term in the cost function to jump out of local minima.

Algorithm 3: Overlapped grouping measurement.

Input : Hamiltonian $\mathbf{O} = \sum_i \alpha_i Q^{(i)}$, the number of samples T .

Output: Estimation v .

- 1 *Generate the initial measurement distribution $\{P^{(s)}, \mathcal{K}_s\}$ with Algorithm 1 or Algorithm 4 ;*
 - 2 *Uniformly randomly pick $A = 10$ groups of distributions $\{\mathcal{K}_s\}$ proportional to $[P^{(s)}, P^{(s)} + \max_s P^{(s)}]$, and choose one with minimum cost function Eq. (15) as the initial point ;*
 - 3 *Find the local optimal distribution $\{P^{(s)}, \mathcal{K}_s\}$ by optimizing the cost function Eq. (15) with Matlab optimization package;*
 - 4 *Sample T measurements from the optimized distribution with Algorithm 2;*
 - 5 *Calculate v with Eq. (8);*
-

We compare the estimation error (averaged over 100 independent tests) using 1000 measurement samples in Table 1. Here the error is estimated with the formula $\varepsilon_v = \sqrt{\frac{1}{N} \sum_{i=1}^N (\hat{v}_i - \text{tr}(\rho O))^2}$. The definition of ε_v is also consistent with the standard deviation calculation of the estimation v . It is worth mentioning that we numerically show that $N = 1000$ independent experiments are sufficient to output a convinced estimation error in Appendix G. We also include the recently proposed derandomized classical shadow method, which is the current state-of-the-art method and has been numerically tested to outperform the others [33]. The numerical result again shows that our OGM method achieves much higher accuracy than other methods when the number of measurements is limited, including the derandomized classical shadow method, verifying its significant performance in the practical computation. The OGM algorithm has simultaneous advantages in the energy estimation under different fermion-to-qubit encodings, including Bravyi-Kitaev (BK) and parity encodings, and we refer to Appendix G for the numerical results and detailed comparison under Bravyi-Kitaev and parity encodings.

Table 1: Estimation errors with 1000 samples for measuring molecular Hamiltonians (JW-encoding) on the corresponding ground states via LDF-grouping, LBCS, derandomized CS, and the OGM method, where the initialized probability for the OGM algorithm is chosen directly from Algorithm 1.

Molecule	LDF	LBCS [27]	Derand [33]	OGM
H ₂ (4)	0.019	0.043	0.018	0.011
H ₂ (8)	0.149	0.128	0.067	0.051
LiH (12)	0.231	0.122	0.063	0.036
BeH ₂ (14)	0.426	0.275	0.103	0.072
H ₂ O (14)	1.090	0.549	0.257	0.129
NH ₃ (16)	1.063	0.484	0.225	0.151

To verify that the OGM method also has advantages when we have a large number of measurements, we show the comparison of the OGM algorithm and LDF Grouping, LBCS, and derandomized CS algorithm for errors with different number of measurements for molecules LiH, and BeH₂ under the JW encoding, as shown in Fig. 2. The results show that the OGM algorithm scales linearly to $1/\sqrt{T}$ for a large number of samples T . This numerical result is consistent with the theoretical results. It can be shown that the OGM algorithm has clear advantages for a large number of samples compared to other existing

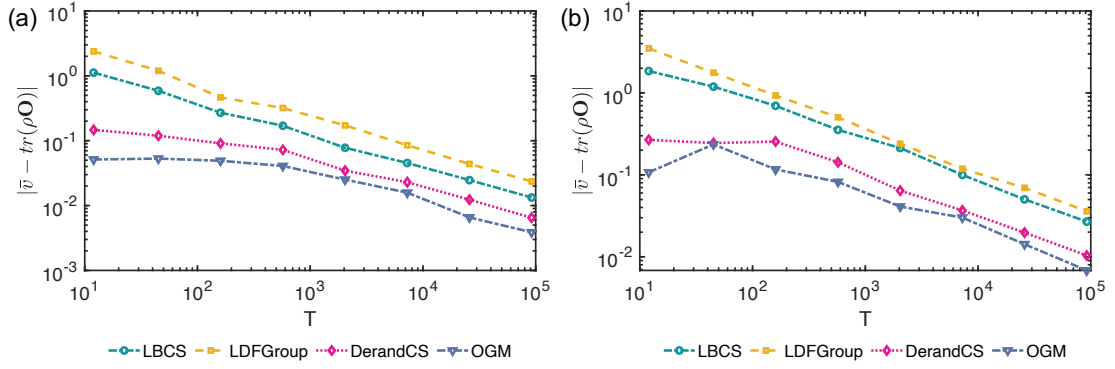


Figure 2: The error of the estimations by the LBCS, LDF Grouping, derandomized CS, and OGM algorithm with the number of measurements for the ground state energy of molecules (a) LiH (12 qubits), and (b) BeH₂ (14 qubits) with JW-encoding.

algorithms. We also provide the comparison of the variances of existing algorithms with OGM algorithm in Appendix F.

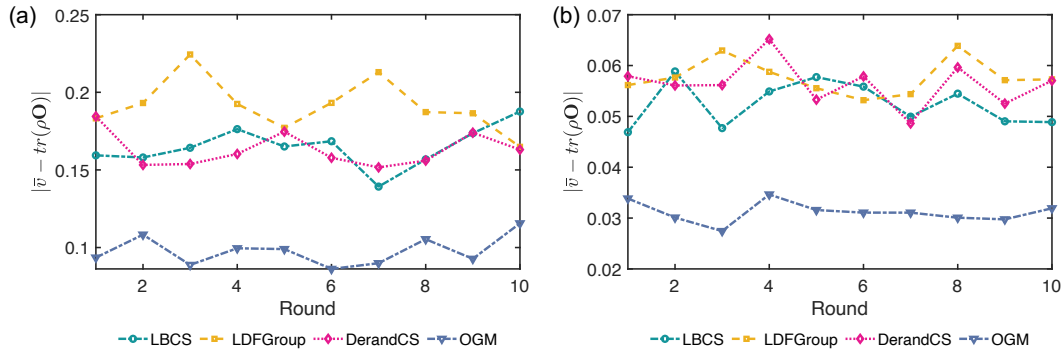


Figure 3: The error of the estimation by the LBCS, LDF Grouping, Derandomized CS and OGM algorithm for the expectation of molecule H₂ (8 qubits) with JW-encoding under 10 random generated 8-qubit state. (a) $T = 1000$ number of samples and (b) $T = 10,000$ number of samples.

We also show Fig. 3 and 4 to illustrate that the advantage of OGM is independent of the quantum input state, where we approximate the expectation of molecule H₂ (8 qubits) with JW-encoding. In Fig. 3, we compare the errors of LBCS, LDF Grouping, Derandomized CS, and OGM algorithms under 10 random generated 8-qubit states with (a) 1000 samples and (b) 10,000 samples. In Fig. 4 we further show the comparison of these algorithms on a randomly generated 8-qubit state with the increase of the number of samples, where the x -axis and the y -axis are both in logarithmic scales. Here we choose the input quantum state as an 8-qubit state with uniformly randomly generated real amplitudes.

We additionally provide the experimental results in Appendix I. The experimental results clearly show a much faster convergence of our OGM method using a few hundred of measurements, which aligns with our theoretical prediction and numerical simulation. We can observe that our methods are practically useful even for the current generation of quantum devices.

6 Discussion and outlook

We introduce a unified framework of quantum measurement that reveals the underlying mechanism of the existing advanced measurement strategies, which are seemingly distinct from each other. We further propose the overlapped grouping measurement (OGM) scheme that integrates the advantages of these typical measurement strategies. Our numerical results suggest a significant improvement over existing advanced measurement methods. Our numerical result shows that our method already demonstrates advantages in practical problems. Since the efficient quantum measurement is crucial for many quantum algorithms and quantum processing, our work has wide applications, such as in variational quantum algorithms and quantum many-body tasks involving eigenenergy estimation [3, 7, 43, 54], where we need to efficiently measure complicated Hamiltonians $\langle H|H \rangle$ or their moments $\langle H^2|H^2 \rangle$ [64]. Our method could significantly reduce the measurement cost and hence speed up the quantum computation, especially when we aim to realize quantum advantage for realistic problems. Moreover, our method applies to adaptive variational quantum simulation, which requires a large number of measurements in each subroutine [25, 75]. It is expected that our measurement scheme will show more advantages with an increasing system size of great practical relevance to both theoretical and experimental tasks.

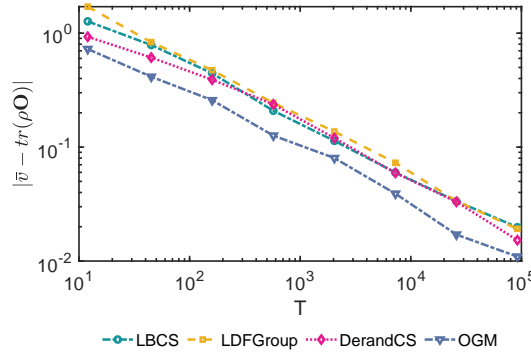


Figure 4: The error of estimation by OGM algorithm for the expectation of molecule H_2 (8 qubits) with JW-encoding under a randomly generated 8-qubit state.

The optimization goal of the OGM algorithm is completely different from the derandomized CS method, since here we utilize a partial variance as the cost function, while the derandomized CS algorithm utilizes a confidence bound. The numerical results also show that our algorithm has clear advantages for a large number of measurements. Our work considers explicit strategies for choosing the overlapped sets, which could be improved using more advanced classical algorithms. Note that the dimension of the considered measurement space is 4^n , and both OGM and CS variant algorithms aim to find a good distribution in this huge space. The expressivity of the CS algorithm is limited since it only explores the $3n$ size of this space. One of the approaches is to combine OGM algorithm with CS for the molecules where parts of qubits have strong correspondence. Briefly speaking, we could utilize the CS method to generate n/s independent subspaces, each grouped with OGM with dimension 4^s . We leave this idea as an interesting future work. Another possible extension is to utilize neural networks to generate samples within the OGM framework [8, 62, 63]. In our work, we assume local Pauli measurements, whereas more general measurements, such as arbitrary local measurements or entangled measurements could be considered [35, 36, 44, 49, 55, 70, 76]. Several measurement schemes have been proposed by adding a polynomial-depth circuit before the local measurement

to implement entangled measurements [24, 34, 70]. How to extend our OGM scheme to generalized measurements is an interesting future direction.

Acknowledgement

We would like to thank Charles Hadfield and Antonio Mezzacapo for providing the Hamiltonians with their work [27] and sharing relevant recent papers. We thank Charles Hadfield, Antonio Mezzacapo, Xiaoming Sun, and Xiaoming Zhang for their helpful discussions. This work is supported by the National Natural Science Foundation of China (Grant No. 12175003, No. 12147133), and Zhejiang Lab’s International Talent Fund for Young Professionals. The numerics is supported by High-performance Computing Platform of Peking University. We acknowledge the use of the IBMQ for this work. The views expressed are those of the authors and do not reflect the official policy or position of IBM or the IBM Q team¹.

Note added.—Recently, two relevant works [26, 30] were posted, which introduce optimized quantum measurement schemes that generalize the classical shadow methods. Hillmich et al. [30] proposed a decision diagrams method to generate an estimation and Hadfield [26] proposed an adaptive Pauli Shadow algorithm to generate an estimation. While similar problems are considered, the techniques are different and could be compared. After our work, Shlosberg et al. [56] and Yen et al. [71] apply the shadow and overlapped grouping ideas to commute measurement respectively, and their results have better performances with the cost of a polynomial-size quantum circuit.

References

- [1] Scott Aaronson. Shadow tomography of quantum states. *SIAM Journal on Computing*, 49(5):STOC18–368, 2019. DOI: [10.1145/3188745.3188802](https://doi.org/10.1145/3188745.3188802). URL <https://doi.org/10.1145/3188745.3188802>.
- [2] Atithi Acharya, Siddhartha Saha, and Anirvan M Sengupta. Informationally complete povm-based shadow tomography, 2021. URL <https://doi.org/10.48550/arXiv.2105.05992>.
- [3] Ryan Babbush, Nathan Wiebe, Jarrod McClean, James McClain, Hartmut Neven, and Garnet Kin-Lic Chan. Low-depth quantum simulation of materials. *Phys. Rev. X*, 8:011044, Mar 2018. DOI: [10.1103/PhysRevX.8.011044](https://doi.org/10.1103/PhysRevX.8.011044). URL <https://doi.org/10.1103/PhysRevX.8.011044>.
- [4] Kishor Bharti, Alba Cervera-Lierta, Thi Ha Kyaw, Tobias Haug, Sumner Alperin-Lea, Abhinav Anand, Matthias Degroote, Hermann Heimonen, Jakob S. Kottmann, Tim Menke, Wai-Keong Mok, Sukin Sim, Leong-Chuan Kwek, and Alán Aspuru-Guzik. Noisy intermediate-scale quantum (nisq) algorithms, 2021. URL <https://doi.org/10.1103/2Frevmodphys.94.015004>.
- [5] Carlos Bravo-Prieto, Ryan LaRose, M. Cerezo, Yigit Subasi, Lukasz Cincio, and Patrick J. Coles. Variational quantum linear solver, 2019. URL <https://doi.org/10.48550/arXiv.1909.05820>.
- [6] Sergey Bravyi, Sarah Sheldon, Abhinav Kandala, David C. McKay, and Jay M. Gambetta. Mitigating measurement errors in multiqubit experiments. *Phys. Rev. A*, 103:

¹The source code for the OGM optimization process is available at <https://github.com/GillianOoO/Overlapped-grouping-measurement>.

- 042605, Apr 2021. DOI: [10.1103/PhysRevA.103.042605](https://doi.org/10.1103/PhysRevA.103.042605). URL <https://doi.org/10.1103/PhysRevA.103.042605>.
- [7] Yudong Cao, Jonathan Romero, Jonathan P. Olson, Matthias Degroote, Peter D. Johnson, Mária Kieferová, Ian D. Kivlichan, Tim Menke, Borja Peropadre, Nicolas P. D. Sawaya, Sukin Sim, Libor Veis, and Alán Aspuru-Guzik. Quantum chemistry in the age of quantum computing. *Chemical Reviews*, 119(19):10856–10915, 2019. DOI: [10.1021/acs.chemrev.8b00803](https://doi.org/10.1021/acs.chemrev.8b00803). URL <https://doi.org/10.1021/acs.chemrev.8b00803>. PMID: 31469277.
 - [8] Juan Carrasquilla, Giacomo Torlai, Roger G Melko, and Leandro Aolita. Reconstructing quantum states with generative models. *Nature Machine Intelligence*, 1(3): 155–161, 2019. DOI: [10.1038/s42256-019-0028-1](https://doi.org/10.1038/s42256-019-0028-1). URL <https://doi.org/10.1038/s42256-019-0028-1>.
 - [9] Marco Cerezo, Andrew Arrasmith, Ryan Babbush, Simon C Benjamin, Suguru Endo, Keisuke Fujii, Jarrod R McClean, Kosuke Mitarai, Xiao Yuan, Lukasz Cincio, et al. Variational quantum algorithms. *Nature Reviews Physics*, 3(9):625–644, 2021. DOI: [10.1038/s42254-021-00348-9](https://doi.org/10.1038/s42254-021-00348-9). URL <https://doi.org/10.1038/s42254-021-00348-9>.
 - [10] Senrui Chen, Wenjun Yu, Pei Zeng, and Steven T. Flammia. Robust shadow estimation. *PRX Quantum*, 2:030348, Sep 2021. DOI: [10.1103/PRXQuantum.2.030348](https://doi.org/10.1103/PRXQuantum.2.030348). URL <https://doi.org/10.1103/PRXQuantum.2.030348>.
 - [11] Kenny Choo, Antonio Mezzacapo, and Giuseppe Carleo. Fermionic neural-network states for ab-initio electronic structure. *Nature communications*, 11(1): 1–7, 2020. DOI: [10.1038/s41467-020-15724-9](https://doi.org/10.1038/s41467-020-15724-9). URL <https://doi.org/10.1038/s41467-020-15724-9>.
 - [12] Cristina Cirstoiu, Zoe Holmes, Joseph Iosue, Lukasz Cincio, Patrick J Coles, and Andrew Sornborger. Variational fast forwarding for quantum simulation beyond the coherence time. *npj Quantum Information*, 6(1):1–10, 2020. URL <https://doi.org/10.1038/s41534-020-00302-0>.
 - [13] J. I. Colless, V. V. Ramasesh, D. Dahlen, M. S. Blok, M. E. Kimchi-Schwartz, J. R. McClean, J. Carter, W. A. de Jong, and I. Siddiqi. Computation of molecular spectra on a quantum processor with an error-resilient algorithm. *Phys. Rev. X*, 8:011021, Feb 2018. DOI: [10.1103/PhysRevX.8.011021](https://doi.org/10.1103/PhysRevX.8.011021). URL <https://doi.org/10.1103/PhysRevX.8.011021>.
 - [14] Benjamin Commeau, M. Cerezo, Zoë Holmes, Lukasz Cincio, Patrick J. Coles, and Andrew Sornborger. Variational hamiltonian diagonalization for dynamical quantum simulation, 2020. URL <https://doi.org/10.48550/arXiv.2009.02559>.
 - [15] Jordan Cotler and Frank Wilczek. Quantum overlapping tomography. *Phys. Rev. Lett.*, 124:100401, Mar 2020. DOI: [10.1103/PhysRevLett.124.100401](https://doi.org/10.1103/PhysRevLett.124.100401). URL <https://doi.org/10.1103/PhysRevLett.124.100401>.
 - [16] Ophelia Crawford, Barnaby van Straaten, Daochen Wang, Thomas Parks, Earl Campbell, and Stephen Brierley. Efficient quantum measurement of pauli operators in the presence of finite sampling error. *Quantum*, 5:385, 2021. DOI: [10.22331/q-2021-01-20-385](https://doi.org/10.22331/q-2021-01-20-385). URL <https://doi.org/10.22331/q-2021-01-20-385>.
 - [17] E. F. Dumitrescu, A. J. McCaskey, G. Hagen, G. R. Jansen, T. D. Morris, T. Papenbrock, R. C. Pooser, D. J. Dean, and P. Lougovski. Cloud quantum computing of an atomic nucleus. *Phys. Rev. Lett.*, 120:210501, May 2018. DOI: [10.1103/PhysRevLett.120.210501](https://doi.org/10.1103/PhysRevLett.120.210501). URL <https://doi.org/10.1103/PhysRevLett.120.210501>.
 - [18] Suguru Endo, Simon C. Benjamin, and Ying Li. Practical quantum error mitigation

- for near-future applications. *Phys. Rev. X*, 8:031027, Jul 2018. DOI: [10.1103/PhysRevX.8.031027](https://doi.org/10.1103/PhysRevX.8.031027). URL <https://doi.org/10.1103/PhysRevX.8.031027>.
- [19] Suguru Endo, Jinzhao Sun, Ying Li, Simon C. Benjamin, and Xiao Yuan. Variational quantum simulation of general processes. *Phys. Rev. Lett.*, 125:010501, Jun 2020. DOI: [10.1103/PhysRevLett.125.010501](https://doi.org/10.1103/PhysRevLett.125.010501). URL <https://doi.org/10.1103/PhysRevLett.125.010501>.
 - [20] Suguru Endo, Zhenyu Cai, Simon C. Benjamin, and Xiao Yuan. Hybrid quantum-classical algorithms and quantum error mitigation. *Journal of the Physical Society of Japan*, 90(3):032001, 2021. DOI: [10.7566/JPSJ.90.032001](https://doi.org/10.7566/JPSJ.90.032001). URL <https://doi.org/10.7566/JPSJ.90.032001>.
 - [21] Keisuke Fujii, Kaoru Mizuta, Hiroshi Ueda, Kosuke Mitarai, Wataru Mizukami, and Yuya O. Nakagawa. Deep variational quantum eigensolver: A divide-and-conquer method for solving a larger problem with smaller size quantum computers. *PRX Quantum*, 3:010346, Mar 2022. DOI: [10.1103/PRXQuantum.3.010346](https://doi.org/10.1103/PRXQuantum.3.010346). URL <https://doi.org/10.1103/PRXQuantum.3.010346>.
 - [22] Joe Gibbs, Kaitlin Gili, Zoë Holmes, Benjamin Commeau, Andrew Arrasmith, Lukasz Cincio, Patrick J. Coles, and Andrew Sornborger. Long-time simulations with high fidelity on quantum hardware, 2021. URL <https://arxiv.org/abs/2102.04313>.
 - [23] Tudor Giurgica-Tiron, Yousef Hindy, Ryan LaRose, Andrea Mari, and William J. Zeng. Digital zero noise extrapolation for quantum error mitigation. In *2020 IEEE International Conference on Quantum Computing and Engineering (QCE)*, pages 306–316, 2020. DOI: [10.1109/QCE49297.2020.00045](https://doi.org/10.1109/QCE49297.2020.00045). URL <https://doi.org/10.1109/QCE49297.2020.00045>.
 - [24] Pranav Gokhale, Olivia Angiuli, Yongshan Ding, Kaiwen Gui, Teague Tomesh, Martin Suchara, Margaret Martonosi, and Frederic T Chong. Minimizing state preparations in variational quantum eigensolver by partitioning into commuting families. URL <https://doi.org/10.48550/arXiv.1907.13623>.
 - [25] Harper R Grimsley, Sophia E Economou, Edwin Barnes, and Nicholas J Mayhall. An adaptive variational algorithm for exact molecular simulations on a quantum computer. *Nature comm.*, 10(1):1–9, 2019. DOI: [10.1038/s41467-018-07090-4](https://doi.org/10.1038/s41467-018-07090-4). URL <https://doi.org/10.1038/s41467-019-10988-2>.
 - [26] Charles Hadfield. Adaptive pauli shadows for energy estimation, 2021. URL <https://doi.org/10.48550/arXiv.2105.12207>.
 - [27] Charles Hadfield, Sergey Bravyi, Rudy Raymond, and Antonio Mezzacapo. Measurements of quantum hamiltonians with locally-biased classical shadows. *Communications in Mathematical Physics*, 391(3):951–967, 2022. DOI: [10.1007/s00220-022-04343-8](https://doi.org/10.1007/s00220-022-04343-8). URL <https://doi.org/10.1007/s00220-022-04343-8>.
 - [28] Cornelius Hempel, Christine Maier, Jonathan Romero, Jarrod McClean, Thomas Monz, Heng Shen, Petar Jurcevic, Ben P. Lanyon, Peter Love, Ryan Babbush, Alán Aspuru-Guzik, Rainer Blatt, and Christian F. Roos. Quantum chemistry calculations on a trapped-ion quantum simulator. *Phys. Rev. X*, 8:031022, Jul 2018. DOI: [10.1103/PhysRevX.8.031022](https://doi.org/10.1103/PhysRevX.8.031022). URL <https://doi.org/10.1103/PhysRevX.8.031022>.
 - [29] Oscar Higgott, Daochen Wang, and Stephen Brierley. Variational Quantum Computation of Excited States. *Quantum*, 3:156, July 2019. ISSN 2521-327X. DOI: [10.22331/q-2019-07-01-156](https://doi.org/10.22331/q-2019-07-01-156). URL <https://doi.org/10.22331/q-2019-07-01-156>.
 - [30] Stefan Hillmich, Charles Hadfield, Rudy Raymond, Antonio Mezzacapo, and Robert Wille. Decision diagrams for quantum measurements with shallow circuits. In *2021 IEEE International Conference on Quantum Computing and Engineering (QCE)*,

- pages 24–34, 2021. DOI: 10.1109/QCE52317.2021.00018. URL <https://doi.org/10.1109/QCE52317.2021.00018>.
- [31] Hsin-Yuan Huang, Richard Kueng, and John Preskill. Predicting many properties of a quantum system from very few measurements. *Nature Physics*, 16(10):1050–1057, 2020. DOI: 10.1038/s41567-020-0932-7. URL <https://doi.org/10.1038/s41567-020-0932-7>.
 - [32] Hsin-Yuan Huang, Kishor Bharti, and Patrick Rebentrost. Near-term quantum algorithms for linear systems of equations with regression loss functions. *New Journal of Physics*, 23(11):113021, nov 2021. DOI: 10.1088/1367-2630/ac325f. URL <https://doi.org/10.1088/1367-2630/ac325f>.
 - [33] Hsin-Yuan Huang, Richard Kueng, and John Preskill. Efficient estimation of pauli observables by derandomization. *Phys. Rev. Lett.*, 127:030503, Jul 2021. DOI: 10.1103/PhysRevLett.127.030503. URL <https://doi.org/10.1103/PhysRevLett.127.030503>.
 - [34] William J Huggins, Jarrod R McClean, Nicholas C Rubin, Zhang Jiang, Nathan Wiebe, K Birgitta Whaley, and Ryan Babbush. Efficient and noise resilient measurements for quantum chemistry on near-term quantum computers. *npj Quantum Information*, 7(1):1–9, 2021. DOI: 10.1038/s41534-020-00341-7. URL <https://doi.org/10.1038/s41534-020-00341-7>.
 - [35] Artur F Izmaylov, Tzu-Ching Yen, Robert A Lang, and Vladyslav Verteletskyi. Unitary partitioning approach to the measurement problem in the variational quantum eigensolver method. *Journal of chemical theory and computation*, 16(1):190–195, 2019. DOI: 10.1021/acs.jctc.9b00791. URL <https://doi.org/10.1021/acs.jctc.9b00791>.
 - [36] Artur F Izmaylov, Tzu-Ching Yen, and Ilya G Ryabinkin. Revising the measurement process in the variational quantum eigensolver: is it possible to reduce the number of separately measured operators? *Chemical science*, 10(13):3746–3755, 2019. DOI: 10.1039/C8SC05592K. URL <https://doi.org/10.1039/C8SC05592K>.
 - [37] Andrew Jena, Scott Genin, and Michele Mosca. Pauli partitioning with respect to gate sets, 2019. URL <https://doi.org/10.48550/arXiv.1907.07859>.
 - [38] Abhinav Kandala, Antonio Mezzacapo, Kristan Temme, Maika Takita, Markus Brink, Jerry M Chow, and Jay M Gambetta. Hardware-efficient variational quantum eigensolver for small molecules and quantum magnets. *Nature*, 549(7671):242–246, 2017. DOI: 10.1038/nature23879. URL <https://doi.org/10.1038/nature23879>.
 - [39] Ying Li and Simon C. Benjamin. Efficient variational quantum simulator incorporating active error minimization. *Phys. Rev. X*, 7:021050, Jun 2017. DOI: 10.1103/PhysRevX.7.021050. URL <https://doi.org/10.1103/PhysRevX.7.021050>.
 - [40] Jin-Guo Liu, Yi-Hong Zhang, Yuan Wan, and Lei Wang. Variational quantum eigensolver with fewer qubits. *Phys. Rev. Research*, 1:023025, Sep 2019. DOI: 10.1103/PhysRevResearch.1.023025. URL <https://doi.org/10.1103/PhysRevResearch.1.023025>.
 - [41] He Ma, Marco Govoni, and Giulia Galli. Quantum simulations of materials on near-term quantum computers. *npj Computational Materials*, 6(1):1–8, 2020. DOI: 10.1038/s41524-020-00353-z. URL <https://doi.org/10.1038/s41524-020-00353-z>.
 - [42] Sam McArdle, Tyson Jones, Suguru Endo, Ying Li, Simon C Benjamin, and Xiao Yuan. Variational ansatz-based quantum simulation of imaginary time evolution. *npj Quantum Information*, 5(1):1–6, 2019. DOI: 10.1038/s41534-019-0187-2. URL <https://doi.org/10.1038/s41534-019-0187-2>.

- [43] Sam McArdle, Suguru Endo, Alán Aspuru-Guzik, Simon C. Benjamin, and Xiao Yuan. Quantum computational chemistry. *Rev. Mod. Phys.*, 92:015003, Mar 2020. DOI: [10.1103/RevModPhys.92.015003](https://doi.org/10.1103/RevModPhys.92.015003). URL <https://doi.org/10.1103/RevModPhys.92.015003>.
- [44] Jarrod R McClean, Jonathan Romero, Ryan Babbush, and Alán Aspuru-Guzik. The theory of variational hybrid quantum-classical algorithms. *New Journal of Physics*, 18(2):023023, feb 2016. DOI: [10.1088/1367-2630/18/2/023023](https://doi.org/10.1088/1367-2630/18/2/023023). URL <https://doi.org/10.1088/1367-2630/18/2/023023>.
- [45] Jarrod R McClean, Mollie E Kimchi-Schwartz, Jonathan Carter, and Wibe A de Jong. Hybrid quantum-classical hierarchy for mitigation of decoherence and determination of excited states. *Physical Review A*, 95(4):042308, 2017. URL <https://doi.org/10.1103/PhysRevA.95.042308>.
- [46] Jarrod R McClean, Zhang Jiang, Nicholas C Rubin, Ryan Babbush, and Hartmut Neven. Decoding quantum errors with subspace expansions. *Nature Communications*, 11(1):1–9, 2020. DOI: [10.1038/s41467-020-14341-w](https://doi.org/10.1038/s41467-020-14341-w). URL <https://doi.org/10.1038/s41467-020-14341-w>.
- [47] Nikolaï Moll, Panagiotis Barkoutsos, Lev S Bishop, Jerry M Chow, Andrew Cross, Daniel J Egger, Stefan Filipp, Andreas Fuhrer, Jay M Gambetta, Marc Ganzhorn, et al. Quantum optimization using variational algorithms on near-term quantum devices. *Quantum Science and Technology*, 3(3):030503, 2018. DOI: [10.1088/2058-9565/aab822](https://doi.org/10.1088/2058-9565/aab822). URL <https://doi.org/10.1088/2058-9565/aab822>.
- [48] Ken M Nakanishi, Kosuke Mitarai, and Keisuke Fujii. Subspace-search variational quantum eigensolver for excited states. *Physical Review Research*, 1(3):033062, 2019. DOI: [10.1103/PhysRevResearch.1.033062](https://doi.org/10.1103/PhysRevResearch.1.033062). URL <https://doi.org/10.1103/PhysRevResearch.1.033062>.
- [49] Bryan O’Gorman, William J Huggins, Eleanor G Rieffel, and K Birgitta Whaley. Generalized swap networks for near-term quantum computing, 2019. URL <https://doi.org/10.48550/arXiv.1905.05118>.
- [50] P. J. J. O’Malley, R. Babbush, I. D. Kivlichan, J. Romero, J. R. McClean, R. Barends, J. Kelly, P. Roushan, A. Tranter, N. Ding, B. Campbell, Y. Chen, Z. Chen, B. Chiaro, A. Dunsworth, A. G. Fowler, E. Jeffrey, E. Lucero, A. Megrant, J. Y. Mutus, M. Neeley, C. Neill, C. Quintana, D. Sank, A. Vainsencher, J. Wenner, T. C. White, P. V. Coveney, P. J. Love, H. Neven, A. Aspuru-Guzik, and J. M. Martinis. Scalable quantum simulation of molecular energies. *Phys. Rev. X*, 6:031007, Jul 2016. DOI: [10.1103/PhysRevX.6.031007](https://doi.org/10.1103/PhysRevX.6.031007). URL <https://doi.org/10.1103/PhysRevX.6.031007>.
- [51] Matthew Otten and Stephen K Gray. Accounting for errors in quantum algorithms via individual error reduction. *Npj Quantum Inf.*, 5(1):11, 2019. DOI: [10.1038/s41534-019-0125-3](https://doi.org/10.1038/s41534-019-0125-3). URL <https://doi.org/10.1038/s41534-019-0125-3>.
- [52] Alberto Peruzzo, Jarrod McClean, Peter Shadbolt, Man-Hong Yung, Xiao-Qi Zhou, Peter J Love, Alán Aspuru-Guzik, and Jeremy L O’Brien. A variational eigenvalue solver on a photonic quantum processor. *Nature comm.*, 5:4213, 2014. DOI: [10.1038/ncomms5213](https://doi.org/10.1038/ncomms5213). URL <https://doi.org/10.1038/ncomms5213>.
- [53] John Preskill. Quantum computing in the nisq era and beyond. *Quantum*, 2:79, 2018. DOI: [10.22331/q-2018-08-06-79](https://doi.org/10.22331/q-2018-08-06-79). URL <https://doi.org/10.22331/q-2018-08-06-79>.
- [54] Google AI Quantum, Collaborators*†, Frank Arute, Kunal Arya, Ryan Babbush, Dave Bacon, Joseph C Bardin, Rami Barends, Sergio Boixo, Michael Broughton, Bob B Buckley, et al. Hartree-fock on a superconducting qubit quantum computer.

- Science*, 369(6507):1084–1089, 2020. DOI: [10.1126/science.abb9811](https://doi.org/10.1126/science.abb9811). URL <https://doi.org/10.1126/science.abb9811>.
- [55] Nicholas C Rubin, Ryan Babbush, and Jarrod McClean. Application of fermionic marginal constraints to hybrid quantum algorithms. *New Journal of Physics*, 20(5):053020, may 2018. DOI: [10.1088/1367-2630/aab919](https://doi.org/10.1088/1367-2630/aab919). URL <https://doi.org/10.1088/1367-2630/aab919>.
 - [56] Ariel Shlosberg, Andrew J. Jena, Priyanka Mukhopadhyay, Jan F. Haase, Felix Leditzky, and Luca Dellantonio. Adaptive estimation of quantum observables, 2021. URL <https://doi.org/10.48550/arXiv.2110.15339>.
 - [57] Armands Strikis, Dayue Qin, Yanzhu Chen, Simon C. Benjamin, and Ying Li. Learning-based quantum error mitigation. *PRX Quantum*, 2:040330, Nov 2021. DOI: [10.1103/PRXQuantum.2.040330](https://doi.org/10.1103/PRXQuantum.2.040330). URL <https://doi.org/10.1103/PRXQuantum.2.040330>.
 - [58] G.I. Struchalin, Ya. A. Zagorovskii, E.V. Kovlakov, S.S. Straupe, and S.P. Kulik. Experimental estimation of quantum state properties from classical shadows. *PRX Quantum*, 2:010307, Jan 2021. DOI: [10.1103/PRXQuantum.2.010307](https://doi.org/10.1103/PRXQuantum.2.010307). URL <https://doi.org/10.1103/PRXQuantum.2.010307>.
 - [59] Jinzhao Sun, Xiao Yuan, Takahiro Tsunoda, Vlatko Vedral, Simon C. Benjamin, and Suguru Endo. Mitigating realistic noise in practical noisy intermediate-scale quantum devices. *Phys. Rev. Applied*, 15:034026, Mar 2021. DOI: [10.1103/PhysRevApplied.15.034026](https://doi.org/10.1103/PhysRevApplied.15.034026). URL <https://doi.org/10.1103/PhysRevApplied.15.034026>.
 - [60] Jinzhao Sun, Suguru Endo, Huiping Lin, Patrick Hayden, Vlatko Vedral, and Xiao Yuan. Perturbative quantum simulation, Sep 2022. URL <https://doi.org/10.1103/PhysRevLett.129.120505>.
 - [61] Kristan Temme, Sergey Bravyi, and Jay M. Gambetta. Error mitigation for short-depth quantum circuits. *Phys. Rev. Lett.*, 119:180509, Nov 2017. DOI: [10.1103/PhysRevLett.119.180509](https://doi.org/10.1103/PhysRevLett.119.180509). URL <https://doi.org/10.1103/PhysRevLett.119.180509>.
 - [62] Giacomo Torlai, Guglielmo Mazzola, Juan Carrasquilla, Matthias Troyer, Roger Melko, and Giuseppe Carleo. Neural-network quantum state tomography. *Nature Physics*, 14(5):447–450, 2018. DOI: [10.1038/s41567-018-0048-5](https://doi.org/10.1038/s41567-018-0048-5). URL <https://doi.org/10.1038/s41567-018-0048-5>.
 - [63] Giacomo Torlai, Guglielmo Mazzola, Giuseppe Carleo, and Antonio Mezzacapo. Precise measurement of quantum observables with neural-network estimators. *Phys. Rev. Res.*, 2:022060, Jun 2020. DOI: [10.1103/PhysRevResearch.2.022060](https://doi.org/10.1103/PhysRevResearch.2.022060). URL <https://doi.org/10.1103/PhysRevResearch.2.022060>.
 - [64] Harish J Vallury, Michael A Jones, Charles D Hill, and Lloyd CL Hollenberg. Quantum computed moments correction to variational estimates. *Quantum*, 4:373, 2020. DOI: [10.22331/q-2020-12-15-373](https://doi.org/10.22331/q-2020-12-15-373). URL <https://doi.org/10.22331/q-2020-12-15-373>.
 - [65] Vladyslav Verteletskyi, Tzu-Ching Yen, and Artur F Izmaylov. Measurement optimization in the variational quantum eigensolver using a minimum clique cover. *The Journal of chemical physics*, 152(12):124114, 2020. DOI: [10.1063/1.5141458](https://doi.org/10.1063/1.5141458). URL <https://doi.org/10.1063/1.5141458>.
 - [66] Samson Wang, Enrico Fontana, Marco Cerezo, Kunal Sharma, Akira Sone, Lukasz Cincio, and Patrick J Coles. Noise-induced barren plateaus in variational quantum algorithms. *Nature communications*, 12(1):1–11, 2021. DOI: [10.1038/s41467-021-27045-6](https://doi.org/10.1038/s41467-021-27045-6). URL <https://doi.org/10.1038/s41467-021-27045-6>.
 - [67] Dave Wecker, Matthew B. Hastings, and Matthias Troyer. Progress towards practical quantum variational algorithms. *Phys. Rev. A*, 92:042303, Oct 2015.

- DOI: 10.1103/PhysRevA.92.042303. URL <https://doi.org/10.1103/PhysRevA.92.042303>.
- [68] Xiaosi Xu, Jinzhao Sun, Suguru Endo, Ying Li, Simon C. Benjamin, and Xiao Yuan. Variational algorithms for linear algebra. *Science Bulletin*, 2021. ISSN 2095-9273. DOI: 10.1016/j.scib.2021.06.023. URL <https://doi.org/10.1016/j.scib.2021.06.023>.
 - [69] Zhi-Cheng Yang, Armin Rahmani, Alireza Shabani, Hartmut Neven, and Claudio Chamon. Optimizing variational quantum algorithms using pontryagin’s minimum principle. *Phys. Rev. X*, 7:021027, May 2017. DOI: 10.1103/PhysRevX.7.021027. URL <https://doi.org/10.1103/PhysRevX.7.021027>.
 - [70] Tzu-Ching Yen, Vladyslav Verteletskyi, and Artur F Izmaylov. Measuring all compatible operators in one series of single-qubit measurements using unitary transformations. *Journal of chemical theory and computation*, 16(4):2400–2409, 2020. DOI: 10.1021/acs.jctc.0c00008. URL <https://doi.org/10.1021/acs.jctc.0c00008>.
 - [71] Tzu-Ching Yen, Aadithya Ganeshram, and Artur F Izmaylov. Deterministic improvements of quantum measurements with grouping of compatible operators, non-local transformations, and covariance estimates, 2022. URL <https://doi.org/10.48550/arXiv.2201.01471>.
 - [72] Xiao Yuan, Suguru Endo, Qi Zhao, Ying Li, and Simon C Benjamin. Theory of variational quantum simulation. *Quantum*, 3:191, 2019. DOI: 10.22331/q-2019-10-07-191. URL <https://doi.org/10.22331/q-2019-10-07-191>.
 - [73] Xiao Yuan, Jinzhao Sun, Junyu Liu, Qi Zhao, and You Zhou. Quantum simulation with hybrid tensor networks. *Phys. Rev. Lett.*, 127:040501, Jul 2021. DOI: 10.1103/PhysRevLett.127.040501. URL <https://doi.org/10.1103/PhysRevLett.127.040501>.
 - [74] Ting Zhang, Jinzhao Sun, Xiao-Xu Fang, Xiao-Ming Zhang, Xiao Yuan, and He Lu. Experimental quantum state measurement with classical shadows. *Phys. Rev. Lett.*, 127:200501, Nov 2021. DOI: 10.1103/PhysRevLett.127.200501. URL <https://doi.org/10.1103/PhysRevLett.127.200501>.
 - [75] Zi-Jian Zhang, Jinzhao Sun, Xiao Yuan, and Man-Hong Yung. Low-depth hamiltonian simulation by adaptive product formula, 2020. URL <https://doi.org/10.48550/arXiv.2011.05283>.
 - [76] Andrew Zhao, Andrew Tranter, William M. Kirby, Shu Fay Ung, Akimasa Miyake, and Peter J. Love. Measurement reduction in variational quantum algorithms. *Phys. Rev. A*, 101:062322, Jun 2020. DOI: 10.1103/PhysRevA.101.062322. URL <https://doi.org/10.1103/PhysRevA.101.062322>.
 - [77] Andrew Zhao, Nicholas C. Rubin, and Akimasa Miyake. Fermionic partial tomography via classical shadows. *Phys. Rev. Lett.*, 127:110504, Sep 2021. DOI: 10.1103/PhysRevLett.127.110504. URL <https://doi.org/10.1103/PhysRevLett.127.110504>.
 - [78] Leo Zhou, Sheng-Tao Wang, Soonwon Choi, Hannes Pichler, and Mikhail D. Lukin. Quantum approximate optimization algorithm: Performance, mechanism, and implementation on near-term devices. *Phys. Rev. X*, 10:021067, Jun 2020. DOI: 10.1103/PhysRevX.10.021067. URL <https://doi.org/10.1103/PhysRevX.10.021067>.

A Sample complexity

In this section, we theoretically analyze the upper bound of the number of copies for the existing algorithms, l_1 -sampling, grouping, and classical shadow algorithm theoretically.

We further provide the variance of the derandomization algorithm and show the relation to our overlapped grouping measurement method.

Let $\hat{v}_1, \dots, \hat{v}_T$ be the estimations after T independent samples. Let $\hat{v} = (\hat{v}_1 + \dots + \hat{v}_T) / T$ be the expectation of these samples. Then by Chebyshev inequality, we have

$$\Pr[|\hat{v} - \text{tr}(\rho Q)| \geq \varepsilon] \leq \frac{\text{Var}(\hat{v})}{\varepsilon^2} = \frac{\text{Var}(\hat{v}_1)}{T\varepsilon^2}. \quad (16)$$

Hence the error can be bounded to ε with probability δ when the number of samples is $\text{Var}(\hat{v}_1) / (\delta\varepsilon^2)$. By the definition of \hat{v} in Eq. (1), the variance of \hat{v} equals $\mathbb{E}[\hat{v}^2] - \text{tr}(\rho \mathbf{O})^2 \leq \mathbb{E}[\hat{v}^2]$.

l₁-sampling.— The variance of \hat{v}_1 generated by l_1 -sampling can be bounded to

$$\text{Var}(\hat{v}_1) \leq \sum_{j=1}^m \alpha_j^2 \frac{\|\alpha\|_1}{|\alpha_j|} = \|\alpha\|_1^2. \quad (17)$$

Hence $T \geq \frac{\|\alpha\|_1^2}{\delta\varepsilon^2}$ suffices to give an estimation with error less than ε and success probability $1 - \delta$.

Grouping.— The variance of \hat{v}_1 generated by grouping method satisfies

$$\begin{aligned} \text{Var}(\hat{v}_1) &\leq \sum_{j,k} \alpha_j \alpha_k f_{\text{Group}}(Q^{(j)}, Q^{(k)}, \mathcal{K}) \text{tr}(\rho Q^{(j)} Q^{(k)}) \\ &\leq \left(\sum_j \alpha_j f_{\text{Group}}(Q^{(j)}, Q^{(j)}, \mathcal{K}) \right)^2 \\ &= \left(\sum_{k=1}^s \frac{1}{\mathcal{K}_j} \sum_{j: Q^{(j)} \in e_k} \alpha_j \right)^2 \\ &= \|\alpha\|_1^2 \left(\sum_{k=1}^s \frac{1}{\|\alpha_{e_k}\|_1} \sum_{j: Q^{(j)} \in e_k} \alpha_j \right)^2, \end{aligned} \quad (18)$$

where $\|\alpha_{e_k}\|_1 = \sum_{j: Q^{(j)} \in e_k} |\alpha_j|$.

Classical shadow.— For classical shadow algorithm, the variance of the generated estimation \hat{v}_1 satisfies

$$\begin{aligned} \text{Var}(\hat{v}_1) &\leq \sum_{j,k} \alpha_j \alpha_k f_{\text{LBCS}}(Q^{(j)}, Q^{(k)}, \mathcal{K}) \text{tr}(\rho Q^{(j)} Q^{(k)}) \\ &\leq \left(\sum_j \alpha_j \prod_{k=1}^n \frac{1}{\chi_k(Q_k^{(j)})} \right)^2 \\ &\leq 3^{\text{local}(\mathbf{O})} \left(\sum_{j=1}^m \alpha_j \right)^2 \end{aligned} \quad (19)$$

where $\text{local}(\mathbf{O}) = \max_{j=1}^m \text{local}(Q^{(j)})$, and the locality of $Q^{(j)}$: $\text{local}(Q^{(j)}) = \#\{k | Q_k^{(j)} \neq \mathbb{I}\}$

is the number of qubits k such that $Q_k^{(j)}$ is not identity. Therefore, $T \geq \frac{3^{\text{local}(\mathbf{O})} \left(\sum_j \alpha_j \right)^2}{\delta\varepsilon^2}$ suffices to give an estimation with error ε and success probability $1 - \delta$.

B LDF Grouping method

In the LDF Grouping method, we mapped the observables and the “compatible with” relationship to a graph. In specific, we denote an observable as a vertex, and if two observables do not have any “compatible with” relationship, we connect them with an edge. Then we can obtain a graph $G(V, E)$, where the number of vertices is equal to m . Next, we can proceed the grouping method as follows.

- (1) Sorting vertices V_1, V_2, \dots, V_m in the descending order of its degree.
- (2) Repeat the following step until all of the vertices are in one of the sets.
- (3) For j goes from 1 to m , if V_j is not in any set, then add $V(j)$ to a set such that there is no edge between $V(j)$ and any other vertices in this set. If such a set does not exist, then add $V(j)$ to a new set.

After the above process and changing V_i into $Q^{(i)}$, we can generate the grouping sets which satisfy any two observables are compatible with each other.

C Greedy overlapped grouping strategy

Aside from the overlapped set generation strategy in Algorithm 1 of the main text, we proposed an alternative strategy that is slightly different in selecting the observables for a set, denoted as Grouping version 2. The main difference is in “the sequence of observables” adding to a new set. The new strategy has a potentially better performance but it needs more time since it has a larger number of sets. We further add a token to each observable to represent how many times we can visit this observable to avoid the explosion of the number of sets. Note that if there is no restriction, the observables in the tail of the sequence will be much more difficult to be added to existing sets, hence the number of sets could be very large.

Let the token of an observable $Q^{(k)}$ be $U_k = 2^{d-1}$, where d is the number of digits of $\lfloor |\alpha_k| / \text{MinWeight} \rfloor$, and $\text{MinWeight} = \min_{j \leq m} |\alpha_j|$ is the minimum weight. This new version of grouping strategy is depicted in Algorithm 4.

We compared the error of the estimation generated by grouping versions 1 and 2 in Table 2. The table shows that when we take more consideration for the observables with larger weight, we have better optimized results, while this would give us a longer optimization time because of the expansion of sets (optimized parameters).

D Variance for the partially derandomized strategy

Suppose that we have determined the measurement basis set \mathcal{M} , in which the number of measurement basis $P^{(k)}$ is assigned as M_k , and the total number of measurements is $T = \sum_k M_k$. We show the variance for the partially derandomized strategy with given measurements T . We denote \mathbf{e}_k containing all $Q^{(k)}$ element-wise commute with basis $P^{(k)}$, and denote s_k as the total number of times that $Q^{(k)}$ is effectively measured, which is given by $s_k = \sum_{P \in \mathcal{M}} \delta_{Q^{(k)} \triangleright P}$. Let $t_{j,k}$ be the measurement outcome of the j th observable $Q^{(j)}$ measured with the basis $P^{(k)}$ is $+1$. The measurement outcome associated with the measurement $P^{(k)}$ for observable $Q^{(j)}$ is thus $\hat{v}_{j,k} = 2t_{j,k}/M_k - 1$. As such, the estimator can be expressed by

$$\hat{v} = \sum_k \hat{v}_k = \sum_k \sum_{j: Q^{(j)} \in \mathbf{e}_k} \frac{\alpha_j M_k}{s_j} \hat{v}_{j,k}. \quad (20)$$

Algorithm 4: Second version of overlapped set generation.

Input : n, m and $Q^{(1)}, \dots, Q^{(m)}, \alpha_1, \dots, \alpha_m, U_1, \dots, U_m$.
Output: $\{P^{(s)}\}$ with initial probabilities $\{\mathcal{K}_s\}$.

- 1 *Sorting all of the observables $\{Q^{(j)}\}$ to the descending order according to their weights $|\alpha_j|$;*
- 2 $j \leftarrow 1$ and $s \leftarrow 1$;
- 3 **while** $\exists Q^{(j)}$ *which is not in any sets :*
- 4 *Let $Q^{(j)}$ be the first observable in the sorted sequence which has never appeared in any sets and add it into a new set e_s ;*
- 5 $s \leftarrow s + 1$;
- 6 *Initialize the measurement of e_s as $P^{(s)} \leftarrow Q^{(j)}$;*
- 7 **for** $k \leftarrow 1$ **to** m **:**
- 8 **if** $Q^{(k)}$ *is compatible with $P^{(s)}$ and $k \neq j$, the number of sets $Q^{(k)}$ appeared is less than token U_k :*
- 9 *Add $Q^{(k)}$ into set e_s , and update $P^{(s)}$ to $P^{(s)} \vee Q^{(k)}$;*
 / $P = Q \vee R$ is defined as $P_i = Q_i$ if $Q_i = R_i$ and $P_i = Q_i R_i$ otherwise. */*
- 10 *Let the initial probability of $P^{(s)}$ be the summation of the weight of all observables in this set;*
- 11 **for** $k \leftarrow 1$ **to** $j - 1$ **:**
- 12 **if** $Q^{(k)}$ *is compatible with $P^{(s)}$ and not in e_s :*
- 13 *Add $Q^{(k)}$ into set e_s , and update $P^{(s)}$ to $P^{(s)} \vee Q^{(k)}$;*

Table 2: Comparison for the errors of the OGM algorithms with grouping version 1 and 2. The error is estimated with 1000 samples for the ground state of the corresponding molecules under JW-encoding.

molecule	H ₂ (4)	H ₂ (8)	LiH	BeH ₂	H ₂ O	NH ₃
error (V1)	0.011	0.051	0.036	0.072	0.129	0.151
error (V2)	0.013	0.047	0.021	0.051	0.121	0.115

One can check that if $M_k > 0$ ($\forall k$) holds, i.e., every observable is assigned at least one measurement basis (one sample), the estimation in Eq. (20) is unbiased.

The variance of the estimator \hat{v} is given by

$$\text{Var}[\hat{v}] = \sum_k M_k \sum_{j,j':Q^{(j)},Q^{(j')} \in \mathcal{S}_k} \frac{1}{s_j s_{j'}} \alpha_j \alpha_{j'} \text{Cov}(\hat{v}_{j,k}, \hat{v}_{j',k}). \quad (21)$$

Here, we use the fact that measurement outcomes obtained from different $P^{(k)}$ are independent since the measurements $P^{(k)}$ are independent of each other. We also note that the outcomes $\hat{v}_{j,k}$ are correlated, so the variance in Eq. (21) depends on the covariance $\text{Cov}(\hat{v}_{j,k}, \hat{v}_{j',k})$.

E Relationship between cost function and variance

Let $o_j := f(P, Q^{(j)}, \mathcal{K}) \mu(P, Q^{(j)})$ be the estimation of $\text{tr}(\rho Q^{(j)})$. The cost function in the manuscript is selected as $\sum_j \alpha_j^2 \mathbb{E}[o_j^2] = \sum_j \alpha_j^2 / \chi(Q^{(j)})$, to evaluate $\text{Var}(v)$. In the following, we prove that $\text{Var}(v) \leq m \sum_j \alpha_j^2 \mathbb{E}[o_j^2]$.

By Eq. (12), we have

$$\text{Var}(\hat{v}) \leq \sum_{j,k} \alpha_j \alpha_k g(Q^{(j)}, Q^{(k)}) \text{tr}(\rho Q^{(j)} Q^{(k)}) \quad (22)$$

$$= \sum_j \alpha_j^2 \mathbb{E}[o_j^2] + \sum_{j \neq k} \alpha_j \alpha_k \frac{\sum_{P: Q^{(j)} \triangleright P, Q^{(k)} \triangleright P} \mathcal{K}(P)}{\chi(Q^{(j)}) \chi(Q^{(k)})} \text{tr}(\rho Q^{(j)} Q^{(k)}) \quad (23)$$

and

$$\sum_{j \neq k} \alpha_j \alpha_k \frac{\sum_{P: Q^{(j)} \triangleright P, Q^{(k)} \triangleright P} \mathcal{K}(P)}{\chi(Q^{(j)}) \chi(Q^{(k)})} \text{tr}(\rho Q^{(j)} Q^{(k)}) \quad (24)$$

$$\leq \sum_{j \neq k} \alpha_j \alpha_k \frac{\sum_{P: Q^{(j)} \triangleright P, Q^{(k)} \triangleright P} \mathcal{K}(P)}{\chi(Q^{(j)}) \chi(Q^{(k)})} \quad (25)$$

$$\leq \sum_{j \neq k} \alpha_j \alpha_k \frac{\min(\chi(Q^{(j)}), \chi(Q^{(k)}))}{\chi(Q^{(j)}) \chi(Q^{(k)})} \quad (26)$$

$$= \sum_{j \neq k} \alpha_j \alpha_k \frac{1}{\max(\chi(Q^{(j)}), \chi(Q^{(k)}))} \quad (27)$$

$$\leq \sum_{j < k} (\alpha_j^2 + \alpha_k^2) \frac{1}{\max(\chi(Q^{(j)}), \chi(Q^{(k)}))} \quad (28)$$

$$\leq (m-1) \sum_j \alpha_j^2 \frac{1}{\chi(Q^{(j)})} \quad (29)$$

$$(30)$$

As shown in Eq. (22), $\mathbb{E}[o_j o_k]$ is associated with the quantum state ρ , and it is unknown for us, while it can be bounded by Eq. (30). Hence we utilize $\sum_j |\alpha_j|^2 \mathbb{E}[o_j^2]$ as our cost function.

F Variance comparison

We compare the variances of different measurement schemes in Table 3, where the initial point is directly chosen from Algorithm 1. Here we generate the measurement distribution by choosing $T = 1000$ in Eq. (15). With a negligible small error ε_0 , we find that our method has a much smaller variance than that of LDF-grouping, and LBCS. The improvement becomes more prominent for larger molecules (approximately one order compared to the classical shadow methods), which indicates its effectiveness for large practical problems with a limited number of measurements.

Table 3: Estimation variances computed on the ground state of the molecular Hamiltonian (under the JW-encoding). The number of qubits is noted in the bracket in the first column, from 4 qubits to 14 qubits. The first 3 columns are the variance of LDF-grouping and OGM algorithms. The last column is the initial error of OGM.

Molecule	variance			ε_0
	LDF	LBCS [27]	OGM	OGM
H ₂ (4)	0.402	1.86	0.424	0
H ₂ (8)	22.3	17.7	5.51	0
LiH (12)	54.2	14.8	3.09	$9.6 \cdot 10^{-5}$
BeH ₂ (14)	135	67.6	15.44	$6.6 \cdot 10^{-4}$
H ₂ O (14)	1040	258	39.64	0.053

G Numerical results and discussions

In this section, we numerically show the advantages of our OGM algorithm compared with l_1 -sampling, LDF Grouping, LBCS, and the derandomized CS algorithm by computing the corresponding variances and errors.

Table 4 shows the comparison of variance of OGM, l_1 -sampling, LDF Grouping, and LBCS algorithms under different fermionic-to-qubit encodings, including JW, bk, and parity encodings. The last column is the deviation of the OGM algorithm after a small perturbation of the cost function as introduced in the main text.

We compare the estimation accuracy with 1000 measurements for molecules H₂, LiH, BeH₂ and H₂O with JW, BK and parity encodings in Table 5, where the initialized probability for the OGM algorithm is chosen directly from Algorithm 1.

H Error of the estimation

We leverage root-mean squared error to quantify the error of the estimation. In each iteration, we generate an estimation \hat{v}_i by independently performing T measurements of initial state ρ . For N independent repetitions, we get the average error of T samples as

$$\varepsilon_v = \sqrt{\frac{1}{N} \sum_{i=1}^N (\hat{v}_i - \text{tr}(\rho O))^2}. \quad (31)$$

We plot the figure to show that the average error will fluctuate in a small range after more than 10 iterations.

In our simulation experiment of the main file (Table 1 and Fig. 2), we choose $N = 100$ for the molecules in which the number of qubits is less than 14. For NH₃ molecule, we let

Table 4: Variance of estimations computed on the ground state of the molecular Hamiltonian with different encoding methods. The first 4 columns are the variance of l_1 -sampling, LDF-grouping, and OGM algorithms. The last column is the corresponding initial error of algorithm OGM.

Molecule	variance				ε_0
	l_1	LDF	LBCS [27]	OGM	OGM
H ₂ (4jw)	2.536	0.402	1.86	0.424	0
H ₂ (4bk)	2.539	0.193	0.541	0.297	0
H ₂ (4parity)	2.539	0.193	0.541	0.297	0
H ₂ (8jw)	119.8	22.3	17.7	5.51	0
H ₂ (8bk)	124.9	38.4	19.5	5.66	$8 \cdot 10^{-6}$
H ₂ (8parity)	124.9	38.0	18.9	6.96	0
LiH (12jw)	145.4	54.2	14.8	3.09	$9.6 \cdot 10^{-5}$
LiH (12bk)	138.5	75.5	68.0	3.53	$1.74 \cdot 10^{-3}$
LiH (12parity)	138.5	85.8	26.5	5.52	$3.03 \cdot 10^{-4}$
BeH ₂ (14jw)	453.4	135	67.6	15.44	$6.6 \cdot 10^{-4}$
BeH ₂ (14bk)	464.9	197	238	17.84	$3.6 \cdot 10^{-3}$
BeH ₂ (14parity)	446	239	130	17.28	$3.42 \cdot 10^{-3}$
H ₂ O (14jw)	4367	1040	258	39.64	0.053
H ₂ O (14bk)	5141	2090	1360	81.59	0.065
H ₂ O (14parity)	5017	2670	429	42.91	0.065

Table 5: Error of estimations with 1000 samples for the ground state of the corresponding molecules with LDF-grouping, LBCS, Derandomized, and OGM algorithms.

Molecule	LDF	LBCS [27]	Derand [33]	OGM
H ₂ (4jw)	0.019	0.043	0.018	0.011
H ₂ (4bk)	0.014	0.025	0.029	0.016
H ₂ (4parity)	0.016	0.016	0.027	0.017
H ₂ (8jw)	0.149	0.128	0.067	0.051
H ₂ (8bk)	0.203	0.143	0.049	0.041
H ₂ (8parity)	0.214	0.138	0.058	0.053
LiH (12jw)	0.231	0.122	0.063	0.036
LiH (12bk)	0.293	0.283	0.067	0.033
LiH (12parity)	0.294	0.145	0.061	0.039
BeH ₂ (14jw)	0.426	0.275	0.103	0.072
BeH ₂ (14bk)	0.462	0.527	0.104	0.082
BeH ₂ (14parity)	0.547	0.355	0.104	0.068
H ₂ O (14jw)	1.090	0.549	0.257	0.129
H ₂ O (14bk)	1.619	1.073	0.274	0.174
H ₂ O (14parity)	1.476	0.708	0.336	0.132
NH ₃ (16jw)	1.063	0.484	0.225	0.151
NH ₃ (16bk)	0.820	0.571	0.282	0.103
NH ₃ (16parity)	2.018	0.663	0.294	0.173

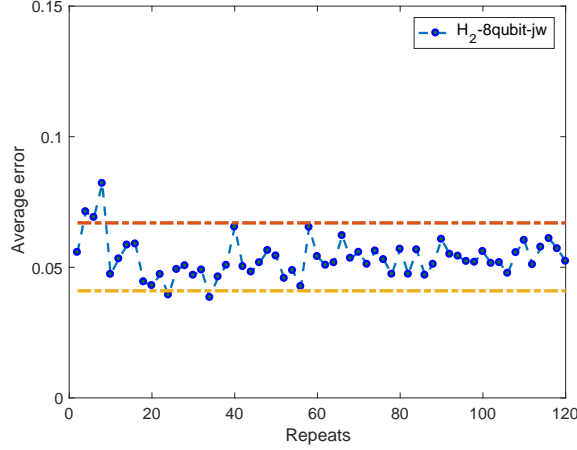


Figure 5: The average errors of different repetitions N for H_2 molecule (8-qubit).

$N = 20$. Nevertheless, the experimental result on the IBM Q device is an average of 12 rounds due to the high cost of the pending time.

I Experimental results

The numerical study ignored device errors, and how the noise in realistic hardware affects the measurement efficiency is critical for studying their practical performance with realistic quantum devices. To further demonstrate the advantage of our OGM method with current quantum devices, we implement and compare the measurement schemes on the IBM quantum cloud hardware with device imperfections. We aim to estimate $\text{tr}(|\psi\rangle\langle\psi|\mathbf{O}_{H_2})$ with the GHZ state $|\psi\rangle = (|0000\rangle + |1111\rangle)/\sqrt{2}$ and the four-qubit Hamiltonian \mathbf{O}_{H_2} of the H_2 molecule under the JW-encoding. We note that the GHZ state has a much larger variance compared to the ground state, and thus could be a suitable testbed to compare the performance of different measurement schemes. In Fig. 6, we compare estimation errors using the l_1 -sampling, LDF-grouping, LBCS, derandomized CS, and the OGM method with a different number of copies (samples) of the prepared entangled state. We evaluate the error by comparing the reference results obtained using the OGM method with 49140 samples.

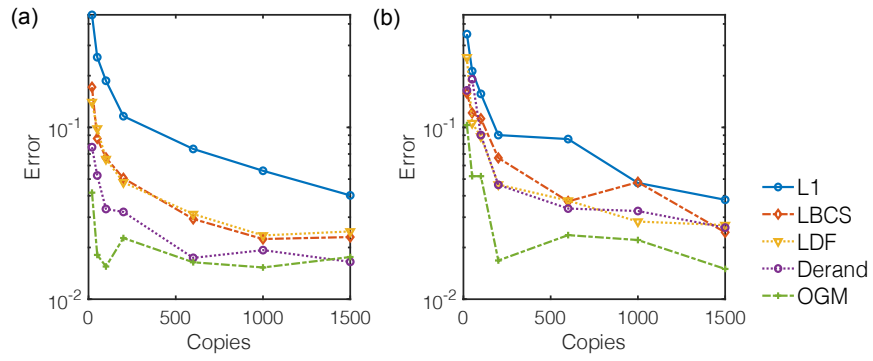


Figure 6: Comparison of OGM with l_1 -sampling, LDF-grouping, LBCS, and derandomized CS using (a) the IBM classical simulator (Repeat 100 rounds) and (b) the IBMQ cloud devices ibmq_athens (Repeat 12 rounds).